

Aluminum based nanostructures for energy applications

Mohammad Tariq Yaseen, Abdalem A. Rasheed

Department of Electrical Engineering, College of Engineering, University of Mosul, Mosul, Iraq

Article Info

Article history:

Received Jul 11, 2020

Revised Sep 20, 2020

Accepted Oct 8, 2020

Keywords:

Aluminum

Nanodisc

Near-Infrared

Plasmonic

ABSTRACT

The plasmonic material properties of aluminum allow active plasmon resonances extending from the blue color in the visible range to the ultraviolet (UV) region of the spectrum. Whereas Al is usually avoided for applications of plasmonics due to its losses in the infrared spectrum region. In this work, the study of the scatter and absorption of disk nanoantennas (DNAs) using various types of materials Au, Ag, and Al is accomplished by using the CST microwave studio suite simulation. The results showed that Al can offer good plasmonic properties when DNA radius is 25 nm to 125 nm at 20 nm height and working wavelengths longer than 800 nm in the near-infrared (NIR) region. Al produces negative plasmonic features around 800 nm wavelength due to the interband transition in the imaginary part of epsilon. For Au and Ag, the plasmonic characteristics rapidly decayed when the DNA radius was higher than 60 nm, but in contrast, Al offers good plasmonic features at these large dimensions of DNAs. This extended response of Al in UV, visible, and NIR, incorporated with its low cost, natural abundance, low native oxide, and amenability to industrial processes, could make Al an extremely promising plasmonic metal candidate for energy applications.

This is an open access article under the [CC BY-SA](#) license.



Corresponding Author:

Mohammad Tariq Yaseen

Department of Electrical Engineering, College of Engineering

University of Mosul

Mosul, Iraq

Email: mtyaseen@uom.edu.iq

1. INTRODUCTION

Metallic nanostructures have been under intensive investigation because of their plasmonic properties and ability to interact with light at subwavelength dimensions [1-3]. Studies of coherent oscillations of electrons in the optical metals, which are recognized as localized surface plasmon resonances (LSPR), were based on the dielectric properties of metals. The resonance wavelength of the plasmonic systems in common depends mainly on the metal nanoparticle size, geometry, and the real and imaginary parts of the dielectric of metal nanoparticles, which are the dispersion properties of the metal [4, 5]. The researchers were highly concentrated on Au and Ag because of their optical and dielectric properties, which could be deployed in different applications. For instance, Ag based nanosensors [6], plasmonic waveguides [7], tunable plasmonic filters [8], nanoantennas for field enhancement [9], nonlinear devices [10], and nanotechnology for energy applications [11, 12].

However, Au and Ag work at wavelengths down to 600 nm. Au is an expensive material, where Ag suffers from rapid oxidation that degrades plasmonic properties. These problems need to be considered when we choose the appropriate material. Even though, Al shows large losses at the interband wavelength around 800 nm. From blue color in the visible region up to the UV region of the spectrum, Al shows low loss and represents a promising plasmonic material [13-15].

As well as, it gives rise to attractive properties that comprise natural abundance, low cost, low native oxide, and ease of processing by the complementary metal-oxide semiconductor (CMOS), whereas Au and Ag do not show the same properties [16]. The absorption enhancement at the near-infrared (NIR) region produces a broadband absorption region [17-19], and then causes a breakthrough in efficiency improvements for solar energy conversion [20-22]. In this paper, Al plasmons of DNAs, as shown in Figure 1, were investigated at the NIR region employing the CST microwave studio simulator based on finite integral technique [23].

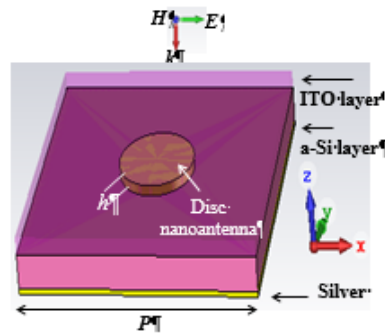


Figure 1. Schematic illustration of the DNA with substrate structure CST

2. RESEARCH METHOD

2.1. Lorentz-drude model

This research work is using Lorentz-Drude model, which is given by as shown in (1) [8]. It shows the dependency of the metal dielectric function on the optical wavelength [3-5].

$$\varepsilon(\omega) = \varepsilon_{int} - \frac{\omega_p^2}{\omega^2 + \gamma^2} + j \frac{\omega_p^2 \gamma}{\omega(\omega^2 + \gamma^2)} \quad (1)$$

$\gamma=1/\tau$ where τ denotes the mean relaxation time of the conduction electrons, and ε_{int} is due to the interband transitions and ω_p is the plasma frequency. The plasmonic metals Au, Ag, and Al have been used as nanoantennas where these metals produce strong field confinement due to the large negative permittivity that produces less field penetration and lower propagation loss [3]. Al plasmonic metal has better plasmonic performance than Au and Ag at short wavelengths such as UV and the blue, due to its low imaginary part and a high negative real part as shown in Figure 2 [10, 20]. In contrast, Al shows large losses at the interband wavelength around 800 nm. Therefore, it is not suitable material for nanoantennas in this region of the spectrum. In infrared wavelengths region, it is true that Al has a higher imaginary part than Au and Ag, but the large value of negative real part of permittivity of Al reduces the field penetration into the plasmonic metal, which gives rise to lower propagation loss in metal and then high field enhancement at the vicinity location of nanoantenna. Also, as shown in Figure 2, Au offers higher loss than Ag at wavelengths below 600 nm that makes Ag better in terms of plasmonic characteristics within this region. Whereas Au is still mostly used because it is chemically very stable [2-4].

2.2. Absorption and scattering calculation model

DNA has been designed and adopted for enhancement of the localized field. Various plasmonic materials were selected such as Au, Ag, and Al. DNA was excited by a plane wave propagating in negative z-direction that is the normal direction to the plane which including the DNA. The symmetry of the circular form of the DNA produces no affectivity to the polarization of incident light. In the first simulation, the DNA was accomplished in the free space without a substrate to investigate the generated scattering (RCS-reflection cross section) and absorption cross section (ACS). It is important to analyze how much of absorption and scattering enhancement can be obtained for Au DNAs, Ag DNAs, and Al DNAs with varying the DNA radius with a constant DNA thickness ($h=20$ nm). The investigation was concentrated on the resonance wavelength attitude, for these important plasmonic metals, with the size variation of DNAs. The resonance wavelength of DNA in the free space relies on the real and imaginary parts of the dielectric constant of the plasmonic metal and the DNAs size. The size of DNA can be controlled whereas the dielectric constant of metal is an inherent characteristic of the metal in shown in (2) and (3), show the relation of the absorption and the scattering with the particle of plasmonic metal that has a radius of a [21, 22]:

$$ACS(\lambda) = \pi a^2 4 \left[\frac{2\pi n_m a}{\lambda} \right] \text{Im} \left[\frac{\varepsilon - \varepsilon_m}{\varepsilon + 2\varepsilon_m} \right] \quad (2)$$

$$RCS(\lambda) = \pi a^2 \frac{8}{3} \left[\frac{2\pi n_m a}{\lambda} \right]^4 \left| \frac{\varepsilon - \varepsilon_m}{\varepsilon + 2\varepsilon_m} \right|^2 \quad (3)$$

where n_m is the refraction index of the surrounding medium, a is the metal sphere radius, ε is the dielectric of the surrounding medium, and ε_m is the plasmonic metal dielectric. It is clear from as shown in (2) and (3) that the ACS and RCS rely on the size and metal type of DNAs, where the ACS related to the a^3 , but the RCS related to the a^6 [17, 18].

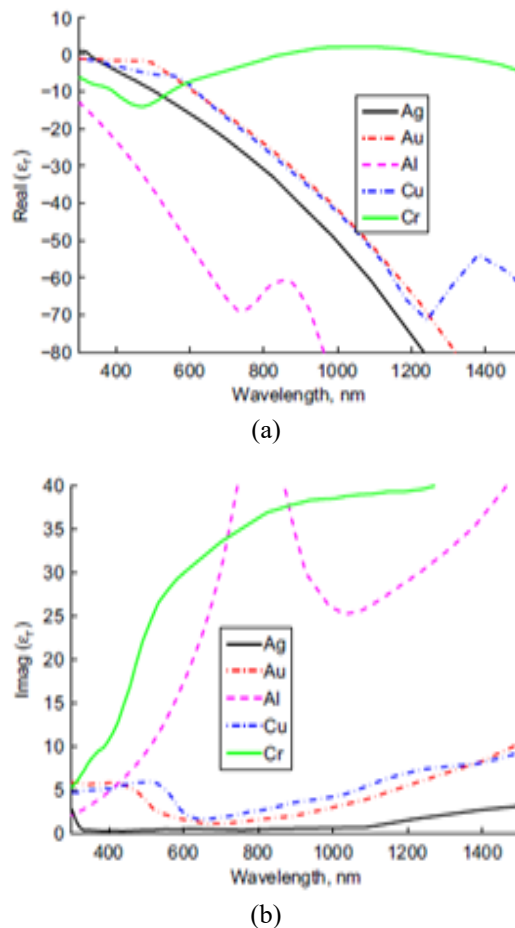


Figure 2. Permittivity of metals using Lorentz-Drude model; (a) real part, (b) imaginary part [20]

3. RESULTS AND ANALYSIS

3.1. Characteristics study of a single DNA in free space

The DNA shown in Figure 1 was simulated as a single DNA in the free space in order to study the behavior, scattering and absorption, with respect to the DNA radius change for different metals. The obtained results are shown in Figure 3. It shows the relation between the RCS and ACS with the DNA radius for plasmonic materials of Au, Ag, and Al. For small dimensions of DNAs, when the $ACS \gg RCS$, it was noticed that the absorption in the DNA will be dominant and the induced electromagnetic field inside the metal will be high. Therefore, this case is not recommended for energy harvesting due to the low field enhancement. However, when the $RCS \gg ACS$, which occurs at large DNAs dimensions, the dominant process induced by DNA is a strong forward scattering of incident radiation. The high forward scattering also reduces the electromagnetic field, where the operation mode is higher than one, which produces high confined field near the DNA. To obtain best localized field enhancement in the DNA, which results in high field enhancement, it is likely to be desirable to operate in a certain size regime and with certain materials for which the RCS is comparable to or slightly higher than the ACS.

In Figure 3 (a), the result of using Ag DNA was shown. It is clear that when the radius was larger than 40 nm, the RCS/ACS ratio increased rapidly with increasing the radius of the DNA. The RCS will be dominant at radii larger than 60 nm. Figure 3 (b) shows the RCS/ACS ratio for Au DNA. The increasing ratio of RCS/ACS with the DNA radius is less than the first case of using Ag DNA. Although, this indicates that Au DNA can be used as a larger diameter than Ag DNA for energy harvesting. Au has a higher imaginary part than Ag that causes the plasmonic deteriorated at a large dimension of particles. This point needs to be considered when using Au material. In Figure 3 (c), the result of using Al DNA was shown. Unlike Au DNA and Ag DNA, Al DNA offers an important feature where the RCS/ACS ratio nearly remains constant at the DNAs radii larger than 55 nm. Not only that, it even tends to decrease at DNAs radii larger than 100 nm. This important matter results in the idea that Al can get over Au and Ag in this wavelength region using certain dimensions of DNAs. This due to the RCS that does not increase rapidly as other metals. However, it is still comparable to or slightly higher than the ACS. This fact is considered an important feature in the energy harvesting applications.

3.2. Characteristics study of a single DNA on a-Si substrate

Here in this section, the DNA shown in Figure 1 was simulated again as a single DNA on a-Si substrate in order to study the resonance wavelengths with respect to the DNA radius change for different metals. The obtained results are shown in Figure 4, shows the relation between the DNA radius and the resonance wavelength for Au DNA, Ag DNA, and Al DNA. Here, the DNAs were mounted on the a-Si substrate of a 60 nm thickness and an indium tin oxide layer of 30 nm. In this simulation, the periodic unit cell in the (x-y direction) was deployed with a 600 nm pitch distance (P), as shown in Figure 1. It was noticed that the resonance wavelength increased (red shifted) with the DNA radius increasing. Also, the extending range of resonance wavelengths for Au, which covers the range from 1000 nm to 3500 nm by radius changing from 20 nm to 80 nm, is lower than Ag and Al. For Ag, the gained response involves the resonance wavelength range from 1000 nm to 6500 nm with radius range from 20 nm to 95 nm. In the case of Al DNA, it is important to notice the slow change of resonance wavelength with respect to the Al DNA radius change. The resonance wavelength extended from 1000 nm to 5000 nm when the Al DNA radius changed from 20 nm to 180 nm.

Figure 5 shows the relation between the DNA radius and absorption in the a-Si layer for various metals. As shown in Figure 5, the absorption was normalized to the maximum value that occurred with the Ag DNA nearly at 55 nm radius. For Au and Ag, the deterioration in the absorption less than 50% occurred at 80 nm and 75 nm, respectively. Whereas for Al, the deterioration in absorption has been occurred at a radius about 140 nm. Also, the maximum absorption in the Al DNA case was a bit lower than the absorption at Ag DNA case. While in the Au DNA case, the absorption is significantly less than other tested metals.

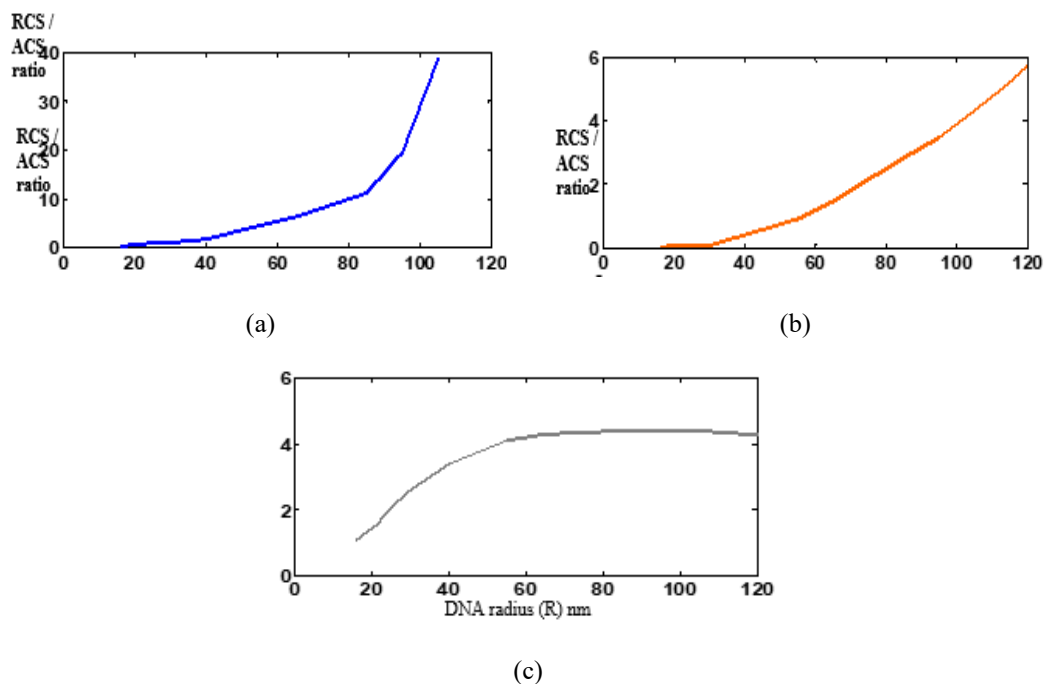


Figure 3. Relation between the DNA radius and RCS/ACS ratio for (a) Ag (b) Au and (c) Al

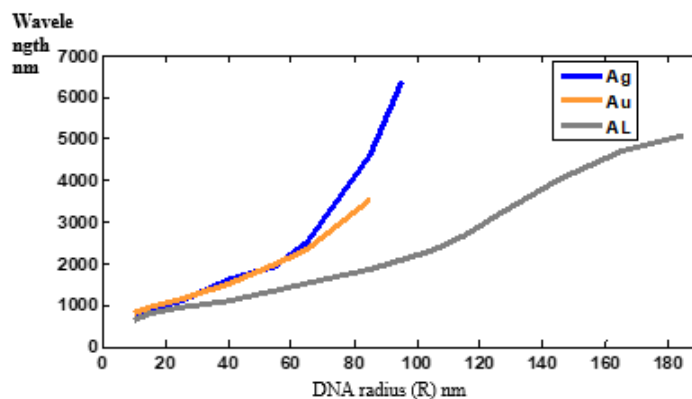


Figure 4. Relation between the DNA radius (R) and resonance wavelengths for Ag,Au, and Al at (h=20 nm)

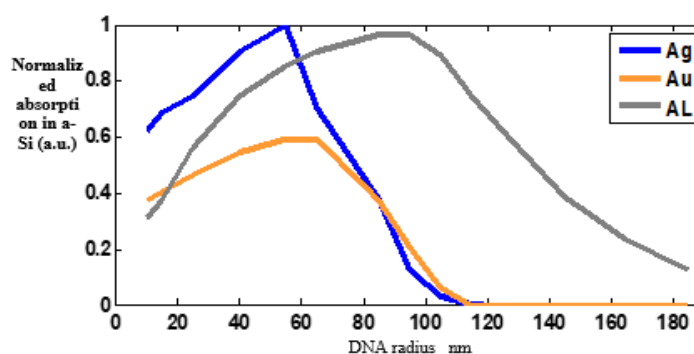


Figure 5. Normalized absorption in a-Si layer at different DNA radii for various metals

Figure 6 represents the results of the normalized absorption in the metal of nanoantenna DNAs that mounted on the a-Si structure for the same radii of Figure 5 and at the resonance wavelength of DNAs. Ag outclasses than other metals at disc radius from 20-60 nm due to its low absorption. When the radius is larger than 60 nm, it was seen that the absorption in Al was higher than Au and Ag. But, it produces better performance for the absorption enhancement in a-Si than other metals. These results confirm that it is true that the Al has a high imaginary part of epsilon which produces high absorption in the plasmonic metal, but it possesses high negative real part at the same time, which results in good plasmonic characteristics at NIR spectrum. Therefore, the results revealed that Al significantly outperformed Au and Ag at wavelength range extended from 1000-5000 nm. Indeed, the Al enables us to overcome the problems of the rapid native oxide of Ag. As well as, these large dimensions of Al nanoantennas DNAs do not need high resolution deposition devices.

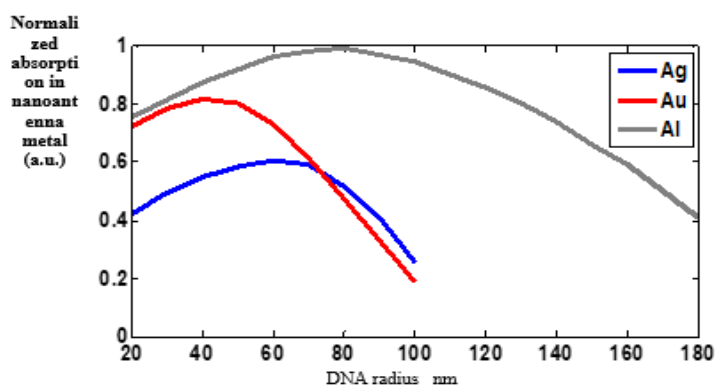


Figure 6. Normalized absorption in the metal of nanoantenna at different DNA radius for various materials types

3.3. Plasmonic resonance mode of a single DNA on a-Si substrate

In this section, DNAs resonate at mode one or more depending on the shape and size. When the size of the DNA is increased, the scattering will increase. "Large particles typically suffer from the presence of multiple nearly degenerate modes that reduce the strength of the fundamental surface plasmon polariton resonance" [11]. Then the issue that must be considered is that the plasmonic order mode to achieve higher localizes field enhancement, which can be found by first-order plasmon exciting [9]. When the DNA size is increased, the higher orders will produce more field oscillation along with the DNA. Then the scattering will be dominant more than the absorption and more plasmonic field confinement will occur in comparison with the first mode. Therefore, to obtain higher localized field enhancement, the focusing keeps on the first mode. Figure 7 shows the field distribution along with the largest DNA. The large DNA has a higher probability than a small size to producing higher modes. To discriminate the first mode, the distribution of the electric field along with the DNA is examined. Figure 7 shows the distribution of the electric field which is negative at the upper half part and positive at the lower half part of DNAs. This electric field distribution points to the first mode of LSPR. The field enhancement using Al is related to photocurrent enhancement from scattering. It could be shown more by the analysis of wavelength dependent photocurrent enhancement [24, 25].

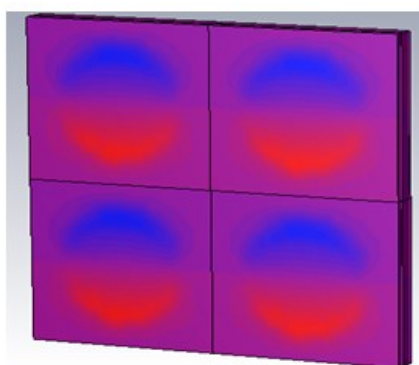


Figure 7. The field distribution along the largest DNA

4. CONCLUSION

Energy applications such as light harvesting are very important currently. However, the cost and efficient materials are still among the challenges for these applications. Plasmonic metals such as Au and Ag have been studied and proposed as good plasmonic materials for the LSPR of metallic nanoparticles at NIR. However, Al based plasmonic structures offer low-cost and promising plasmonic properties for light harvesting. In this work, the potential of Al plasmonic metal of DNAs to support strong LSPR at NIR is investigated and demonstrated by examining the behavior of the scattering and absorption cross-section with a DNA radius. The aim of using disc form is to obtain a similarity response to the applied E-field due to its circular shape. The cross-section of absorption and scattering of Al DNAs are compared with Au and Ag DNAs for the same dimensions. These results make Al outperformed in LSPR and good absorption in the substrate at wavelengths longer than 800 nm and NIR spectral range that extended from 1000 nm to 5000 nm, which gives an alternative to other plasmonic noble metals. Ultimately, it can join the NIR region to extend the active plasmonic range of Al from UV, visible, to the NIR spectrum range and enables a various and tailorable platform of plasmon-enhanced light harvesting applications.

ACKNOWLEDGEMENTS

The authors are very grateful to the University of Mosul, College of Engineering for their provided facilities, which helped to improve the quality of this work.

REFERENCES

- [1] D. Franklin, *et al.*, "Self-assembled plasmonics for angle-independent structural color displays with actively addressed black states," *PNAS*, vol. 117, no. 24, pp. 1335-1335, Jun. 2020.
- [2] Junxi Zhang, Lide Zhang, "Nanostructures for surface plasmons," *Adv. Opt. Photon.*, vol. 4, pp. 157-321, Jun. 2012.
- [3] P. R. West, *et al.*, "Searching for better plasmonic materials," *Laser Photonics Rev.*, vol. 4, no. 6, pp. 795-808, 2010.

- [4] S. Babar and J. H. Weaver, "Optical constants of Cu, Ag, and Au revisited," *Appl. Opt.*, vol. 54, no. 3, pp. 477-481, 2015.
- [5] Y. Li and Y. Li, "Optical properties of plasmonic materials," *Plasmonic Opt. Theory Appl.*, 2017.
- [6] J. C. Reed, H. Zhu, A. Y. Zhu, C. Li, and E. Cubukcu, "Graphene-enabled silver nanoantenna sensors," *Nano Lett.*, vol. 12, no. 8, pp. 4090-4094, 2012.
- [7] A. V. Krasavin and A. V. Zayats, "Silicon-based plasmonic waveguides," *Opt. Express*, vol. 18, no. 11, pp. 11791-11799, 2010.
- [8] A. Setayesh, S. R. Mirnaziry, and M. S. Abrishamian, "Numerical Investigation of tunable band-pass band-stop plasmonic filters with hollow-core circular ring resonator," *Journal of the Optical Society of Korea*, vol. 15, no. 1, pp. 82-89, 2011.
- [9] B. S. Archanjo, *et al.*, "Plasmon 3D electron tomography and local electric-field enhancement of engineered plasmonic nanoantennas," *ACS Photonics*, vol. 5, no. 7, pp. 2834-2842, May 2018.
- [10] O. Rectification, F. Generation, and X. Lei, "Nonlinear metal-insulator-metal (MIM) nanoplasmonic waveguides based on electron tunneling for optical rectification and frequency generation," *MSc. thesis, Univ. Alberta*, 2013.
- [11] L. Tsakalagos, *Nanotechnology for Photovoltaics*, CRC Press Taylor & Francis Group, 1st ed., October 20, 2019, p. 458.
- [12] M. T. Yaseen, F. Y. Abdullah and M. H. Almallah, "Smart Green Farm," *2020 7th International Conference on Electrical and Electronics Engineering (ICEEE)*, pp. 299-302, Apr. 2020.
- [13] M. W. Knight, *et al.*, "Aluminum for plasmonics," *ACS Nano*, vol. 8, no. 1, pp. 834-840, 2014.
- [14] R. M. Altuwirqi, B. Baatayah, E. Nugali, Z. Hashim, H. Al-Jawhari, "Synthesis and characterization of aluminum nanoparticles prepared in vinegar using a pulsed laser ablation technique," *Journal of Nanomaterials*, pp. 5, 2020.
- [15] O. Lecarme, Q. Sun, K. Ueno, and H. Misawa, "Robust and versatile light absorption at near-infrared wavelengths by plasmonic aluminum nanorods," *ACS Photonics*, vol. 1, no. 6, pp. 538-546, 2014.
- [16] L. Tang, S. Latif, and D. A. B. Miller, "Plasmonic device in silicon CMOS," *Electron. Lett.*, vol. 45, no. 13, pp. 706-708, 2009.
- [17] C. F. Bohren and D. R. Huffman, "Absorption and scattering of light by small particles," *John Wiley & Sons, New York: John Wiley & Sons*, 2008.
- [18] Kondorskiy, A. D., Lam, N. T. & Lebedev, V. S., "Absorption and Scattering of Light by Silver and Gold Nanodisks and Nanoprisms," *Journal of Russian Laser Research*, vol. 39, pp. 56-66, 2018.
- [19] Petoukhoff, C., O'Carroll, D., "Absorption-induced scattering and surface plasmon out-coupling from absorber-coated plasmonic metasurfaces," *Nature Communication*, vol. 6, no. 7899, 2015.
- [20] G. A. E. Vandenbosch and Z. Ma, "Upper bounds for the solar energy harvesting efficiency of nano-antennas," *Nano Energy*, vol. 1, no. 3, pp. 494-502, May 2012.
- [21] S.-W. Baek, *et al.*, "Plasmonic forward scattering effect in organic solar cells: a powerful optical engineering method," *Scientific Reports*, vol. 3, pp. 1726-1733, 2013.
- [22] D. Derkacs, S. H. Lim, P. Matheu, W. Mar, and E. T. Yu, "Improved performance of amorphous silicon solar cells via scattering from surface plasmon polaritons in nearby metallic nanoparticles," *Applied Physics Letters*, pp. 239-241, Aug. 2006.
- [23] *CST Studio Suite 3D EM simulation and analysis software*, 3DS Simula [Online]. Available: https://www.3ds.com/products-services/simulia/products/cst-studio-suite/?utm_source=cst.com&utm_medium=301&utm_campaign=cst.
- [24] Wang L., Yan Y., Ji X., "Improving the energy conversion efficiency of a laser-driven flyer by an in situ-fabricated nano-absorption layer," *Nanoscale Res Lett*, vol. 15, no. 1, Dec. 2020.
- [25] Mehrnoosh Saleemizadeh, Fatemeh Fouladi Mahani, and Arash Mokhtari, "Design of aluminum-based nanoring arrays for realizing efficient plasmonic sensors," *Journal of the Optical Society of America B*, vol. 36, no. 3, pp. 786-793, Mar. 2019.